applied sciences

MDPI

Article

Study on Fatigue Characteristics and Interlayer Design Method of Waterproof Cohesive Bridge Deck Layer

Naren Fang [1,*], Xuancang Wang [1,*], Hongyu Ye [1], Yaoning Sun [1], Ziyuan Su [2] and Lun Yuan [3]

1 School of Highway Engineering, Chang'an University, Xi'an 710064, China; 2017021035@chd.edu.cn (H.Y.); syn20159@163.com (Y.S.)
2 Road and Bridge Branch of Henan Institute of Urban Planning and Design, Henan 450000, China; 119912488@163.com
3 China Communications Construction Group First Highway Consultants CO.LTD, Xi'an 710064, China; zlyy2339@hotmail.com
* Correspondence: 2017021044@chd.edu.cn (N.F.); wxc2005@chd.edu.cn (X.W.); Tel.: +86-029-8233-4836 (X.W.)

Received: 9 April 2019; Accepted: 13 May 2019; Published: 21 May 2019

check for updates

Abstract: Shear fatigue damage to the waterproof cohesive layer has not received enough attention in bridge deck pavement design. Meanwhile, there is less theoretical basis for the design of a waterproof cohesive layer. In this study, direct shear and shear fatigue tests were used to compare the shear strength and fatigue performance of waterproof adhesive materials under different disposal schemes for a cement slab surface, bonding materials, and spreading schemes, and the recommended optimal dosage of waterproof adhesive material for the bridge deck is given. Based on the shear fatigue tests results of indoor waterproof adhesive materials, an equation for prediction fatigue at 15 °C was established and temperature correction was applied. Based on these results, we propose a waterproof cohesive layer design method for bridge deck pavement with interlayer shear damage as the design index. The life expectancy of the shear damage between the decks was calculated for a real bridge deck. These results provide scientific guidance for design of a waterproof cohesive layer in a bridge deck, which can effectively extend the service life of a bridge deck.

Keywords: bridge deck engineering; waterproof cohesive layer; fatigue equation; shear fatigue damage; interlayer design

1. Introduction

At present, most bridge deck pavement structures use a "concrete slab + asphalt concrete" pavement system. Cement concrete pavement is initially poured, and asphalt concrete is then paved over the surface of the cement concrete pavement to form a rigid-flexible composite structure [1]. The waterproof cohesive layer ensures the bridge remains waterproof, and the rigid-flexible structure layer is bonded together. As an important part of the bridge deck pavement structure, improperly setting the waterproof cohesive layer will result in an insufficient interlayer bonding force or shear strength, ultimately damaging the overall pavement structure [2]. Therefore, it is particularly important to study the shear fatigue characteristics of the waterproof cohesive layer.

Many scholars have focused their research on the deck pavement's construction and the waterproof material [3–6]. Some scholars have studied the effect of construction temperature on interlayer cohesion. For example, results from a TRRL [7] test in Britain showed that using an asphalt mixture in paving will damage the waterproof cohesive layer, thus affecting affects its performance. West et al. [8] showed that the shear strength of the waterproof cohesive layer decreases as the temperature increases. Ye et al. [9] used grey correlation to determine correlations among various factors that influence the shear strength of the waterproof cohesive layer. Some scholars have developed new waterproof cohesive layer materials to improve the shear strength of bridge deck pavement. For example, Song et al. [10] improved the cohesive force of a waterproof material by incorporating a latex modifier similar to the emulsion and proposed an optimum coating thickness of 0.7–1 mm. Lv et al. [11] developed a macromolecule polymer bitumen waterproof cohesive layer that is suitable for hot, humid regions. Wang [12] developed a new epoxy-modified asphalt waterproof adhesive material with bond strength reaching 0.6 MPa, which greatly increased the bonding strength of the bridge deck waterproof cohesive layer. Wang et al. [13] developed a high-performance polymer bridge deck waterproof adhesive material with 0.5 MPa shear strength at 25 °C and 0.0885 MPa at 60 °C. Other scholars studied the shear resistance and fatigue life of the waterproof cohesive layer. The research of Ji et al. [14] showed that the primary factor determining the shear strength is the interaction between the rubber asphalt and the concrete surface. Rhee et al. [15] used a French pavement design procedure to analyze the stress on the pavement between different layers and found that insufficient contact between layers may reduce the service life to 65–70% of the design life.

In summary, although many scholars have studied the waterproof cohesive layer with different test methods, evaluation indicators, and standards, there are still some shortcomings [16–19]. For example, the interlayer construction method and material are rarely considered together, and the development of new materials is costly and difficult to apply. There is no unified standard regarding the content of relevant materials used in the waterproof cohesive layer. The initial stage of fatigue damage in the waterproof cohesive layer is difficult to observe, and research on shear fatigue damage to a waterproof cohesive layer in a bridge deck is lacking.

The common waterproof synchronous gravel cohesive layer, shear strength of different disposal schemes for a cement slab, bonding materials, and different combinations of spreading schemes were examined and compared in this study. The optimum material composition (which corresponds to the maximum shear strength in different test schemes.) of the waterproof cohesive layer for a bridge deck is presented based on comprehensive consideration of various interlayer construction methods and materials. The shear fatigue characteristics of different bridge deck waterproof adhesive materials were studied, and a model for predicting the fatigue life is presented. A method for designing the waterproof cohesive layer for a bridge deck based on shear fatigue damage to the interlayer materials is proposed.

2. Performance Test of Waterproof Cohesive Layer Material

2.1. Test Plans

Basalt (4.75–9.5 mm) was selected as a gravel material, and 27 shear test schemes were used to analyze the bonding material, spreading scheme, and shear resistance of a waterproof cohesive material in different cement slab surface disposal schemes. The 27 test schemes are shown in Table 1.

The "AC-13+waterproof cohesive layer + cement concrete slab" structure was used in the indoor shear test of the bridge deck interlayer materials. A $150 \times 150 \times 150$ mm^3 cement concrete slab was fabricated and the slab surface was disposed (brushed cement concrete, grooved cement concrete, exposed aggregate cement concrete). After 7 days of maintenance under standard conditions, core samples were drilled with a 100 mm diameter core drill. Waterproof cohesive layers were laid on the surface of the cement concrete core samples with different asphalt and gravel content. Finally, the core samples were loaded into a 101.6×87 mm^2 Marshall test model, and a hot mix AC-13 asphalt mixture was loaded into the test model. The model was compacted with a compactor and formed after the asphalt surface was allowed to cool. The test model was removed, and a direct shear test was conducted. The forming and testing process of shear samples are shown in Figure 1.

Table 1. Composition of 27 test schemes.

Asphalt Type	Spreading Scheme	Disposal Scheme of Cement Slab Surface	Test Scheme
SBS-modified emulsified asphalt	A	brushed cement concrete	Emu-A-brushed
		grooved cement concrete	Emu-A-grooved
		exposed aggregate cement concrete	Emu-A-exposed
	B	brushed cement concrete	Emu-B-brushed
		grooved cement concrete	Emu-B-grooved
		exposed aggregate cement concrete	Emu-B-exposed
	C	brushed cement concrete	Emu-C-brushed
		grooved cement concrete	Emu-C-grooved
		exposed aggregate cement concrete	Emu-C-exposed
90 ordinary hot asphalt	A	brushed cement concrete	Ord-A-brushed
		grooved cement concrete	Ord-A-grooved
		exposed aggregate cement concrete	Ord-A-exposed
	B	brushed cement concrete	Ord-B-brushed
		grooved cement concrete	Ord-B-grooved
		exposed aggregate cement concrete	Ord-B-exposed
	C	brushed cement concrete	Ord-C-brushed
		grooved cement concrete	Ord-C-grooved
		exposed aggregate cement concrete	Ord-C-exposed
SBS-modified asphalt	A	brushed cement concrete	Mod-A-brushed
		grooved cement concrete	Mod-A-grooved
		exposed aggregate cement concrete	Mod-A-exposed
	B	brushed cement concrete	Mod-B-brushed
		grooved cement concrete	Mod-B-grooved
		exposed aggregate cement concrete	Mod-B-exposed
	C	brushed cement concrete	Mod-C-brushed
		grooved cement concrete	Mod-C-grooved
		exposed aggregate cement concrete	Mod-C-exposed

Spreading scheme A: Asphalt is first sprayed on the road surface, then gravel is sprayed, and a single waterproof cohesive layer is formed by rolling; Spreading scheme B: Asphalt is first sprayed on the road surface, then crushed stone wrapped with hot asphalt is sprayed, and a single waterproof cohesive layer is formed by rolling; Spreading scheme C: Asphalt is first sprayed on the road surface, then gravel is sprayed, followed by a layer of asphalt, yielding a double waterproof cohesive layer after rolling; Brushed cement concrete: Before setting the initial cement concrete board, wet cotton cloth was used to form a texture on the surface of the cement board with a depth of approximately 3 mm; Grooved cement concrete: Grooves (5 mm width, 3 mm depth, and 10 mm spacing) were placed on the surface of cement concrete board; Exposed aggregate cement concrete: When the cement concrete board was not hardened, the surface mortar is removed to expose approximately 1 mm of coarse aggregate.

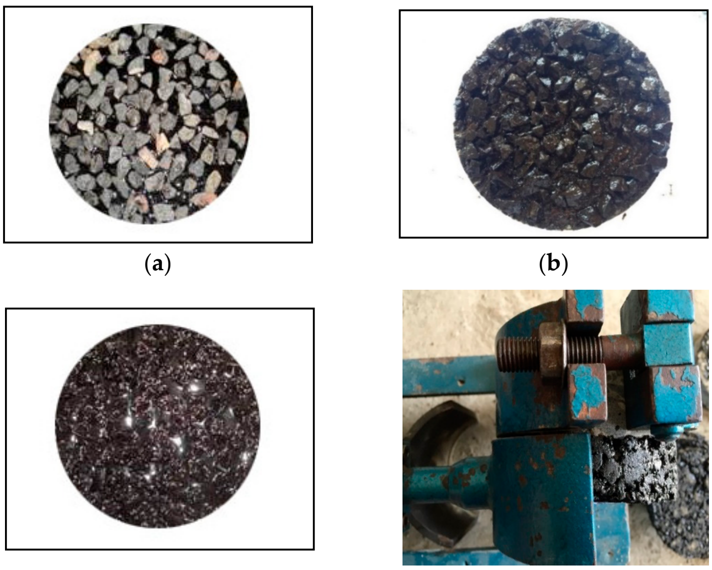

(**a**) (**b**) (**c**) (**d**)

Figure 1. The forming and testing process of shear samples with different spreading schemes: (**a**) the sample forming process of Spreading scheme A; (**b**) the sample forming process of Spreading scheme B; (**c**) the sample forming process of Spreading scheme C; and (**d**) the Shear test process.

2.2. Material Design

2.2.1. Tack Coat Material Design

The research of Zhang et al. [20] shows that the increase of ductility and plasticity of interlayer waterproof materials will lead to the increase of compactness of materials. Therefore, the contact between materials and cement concrete slabs is close and the water proof performance under moving repeated loading is good. Experimental results and technical specifications for the different materials in the SBS-modified emulsified asphalt, 90 ordinary hot asphalt, and SBS-modified asphalt are shown in Tables 2–4.

Table 2. Technical indices of SBS-modified emulsified asphalt.

Pilot Project	Unit	Testing Value	Standard
Emulsion stability velocity	—	Quick	Quick or median split
Particle charge	—	Cation (+)	Cation (+)
Weight of screen residue (1.18 mm)	%	0.07	≤0.1
Engler viscosity E25	—	6	1-10
Asphalt standard viscosity C25	S	13	8-25
Evaporation residue content	%	54	≤50
Penetration (100 g, 25 °C, 5 s)	0.1 mm	62	40–120
Softening point	°C	55.7	≤50
Ductility (5 °C)	0.1 mm	37	≥20
Solubility (TCE)	°C	98.6	≥97.5
Storage stability 1 d	%	0.5	1
Storage stability 5 d	%	1.4	5

Table 3. Technical indices of 90 ordinary hot asphalt.

Pilot Project	Unit	Testing Value	Standard
Penetration 25 °C, 100 g, 5 s	0.1 mm	95	80~100
Penetration index (PI)	—	−1.04	−1.5~+1.0
Softening point TR&B	°C	45.0	≥44
Dynamic viscosity (60 °C)	Pa·s	147	≥120
Ductility(10 °C, 5 cm/min)	cm	/	/
Ductility(15 °C, 5 cm/min)	cm	>140	≥100
Wax content	%	1.2	≤2.2
Flash point	°C	≥230	≥245
Solubility	%	99.9	≥99.5

Table 4. Technical indices of SBS-modified asphalt.

Pilot Project	Unit	Testing Value	Standard
Penetration 25 °C, 100 g, 5 s	0.1 mm	71	60~80
Penetration index (PI)	—	0.057	≥−0.4
Softening point TR&B	°C	66	≥55
Dynamic viscosity (135 °C)	Pa·s	2.5	≤3
Ductility (5 °C, 5 cm/min)	Cm	42	≥30
Flash point	°C	265	≥230
Solubility	%	99.7	≥99
Elastic recovery (25 °C)	%	95	≥65

2.2.2. Design of Cement Concrete

The cement concrete mix used in the test is shown in Table 5.

Table 5. Mix proportion of cement concrete.

Ingredient	Cement	Expansive Agent	Sand	Fine Aggregate	Coarse Aggregate	Water	Admixture	Steel Fiber
Proportion (kg/m^3)	440	38	761	404	605	172	5.736	50

2.2.3. Design of Asphalt Concrete

The composition of the AC-13 asphalt surface material is shown in Table 6.

Table 6. Aggregate gradation.

Type of the Mixture	Passing Percentage (%)											Optimum Asphalt Content
	19.0	16.0	13.2	9.5	4.75	2.36	1.18	0.6	0.3	0.15	0.075	
AC-13	100	100	92	70	40.3	31.5	25.4	19.2	12.7	9.2	5.9	4.9%

2.3. Testing Procedure and Result

2.3.1. SBS-Modified Emulsified Asphalt

SBS-modified emulsified asphalt was sprayed with areal densities of 0.8, 1.0, 1.2, 1.4, and 1.6 kg/m^2, and gravel was sprayed with areal densities of 5.0, 6.0, 7.0, and 8.0 kg/m^2, yielding a total of 20 waterproof materials. According to the test scheme Emu-A-brushed, Emu-A-grooved, Emu-A-exposed, Emu-B-brushed, Emu-B-grooved, and Emu-B-exposed, each type of adhesive material specimen was prepared and tested using a direct shear test (please refer to Table 1 for details). The experimental results are shown in Figure 2, and the amount of asphalt and gravel content corresponding to the maximum shear strength is taken as optimum.

Figure 2 shows that the optimum asphalt content in scheme Emu-A-brushed, Emu-A-grooved, Emu-B-brushed, and Emu-B-grooved is 1.2 kg/m^2, and the optimum gravel content is 6.0 kg/m^2. The optimum asphalt content of scheme Emu-A-exposed and Emu-B-exposed is 1.4 kg/m^2, and the optimum stone content is 7.0 kg/m^2. The shear strength of the waterproof cohesive layer initially increases, and then decreases as the gravel content increases. This is because increasing the amount of gravel will increase interlaminar compression when the amount of asphalt is fixed. When the amount of aggregate reaches a critical point, a continuous increase in aggregate will cause bonding damage, which will decrease the interlaminar shear strength.

After determining the optimum amount of asphalt and gravel content in scheme A, the upper asphalt was sprayed with areal density of 0.2, 0.4, 0.6, 0.8, or 1.0 kg/m^2, which is composed of five kinds of waterproof adhesives material. According to the test scheme Emu-C-brushed, Emu-C-grooved, and Emu-C-exposed, each kind of waterproof adhesive material was prepared and direct shear tests were carried out (please refer to Table 1 for details). The test results are shown in Figure 3, and the amount of sprayed asphalt content corresponding to maximum shear strength is taken as optimum.

Figure 3 shows that the optimum asphalt content in the upper modified asphalt in scheme Emu-C-brushed, Emu-C-grooved, and Emu-C-exposed is 0.6 kg/m^2. The best asphalt content in scheme Emu-C-brushed and scheme Emu-C-grooved is 0.6 kg/m^2 for the upper layer and 1.2 kg/m^2 for the lower layer, with 6.0 kg/m^2 for gravel content. The best asphalt content in scheme Emu-C-exposed is 0.6 kg/m^2 for the upper layer and 1.4 kg/m^2 for the lower layer, with 7.0 kg/m^2 for gravel content.

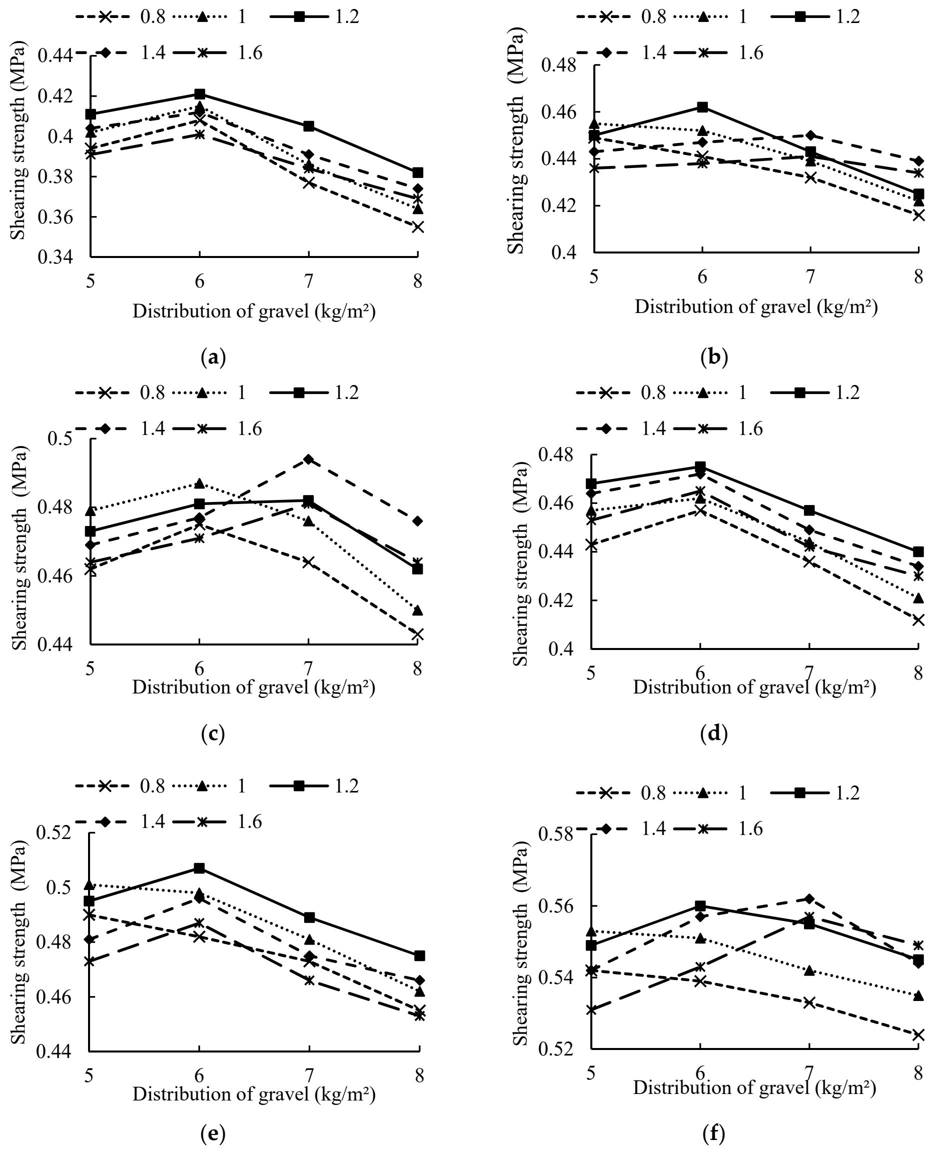

Figure 2. Shear strength of SBS-modified emulsified asphalt with different spreading and disposal schemes: (**a**) Emu-A-brushed; (**b**) Emu-A-grooved; (**c**) Emu-A-exposed; (**d**) Emu-B-brushed; (**e**) Emu-B-grooved; (**f**) Emu-B-exposed.

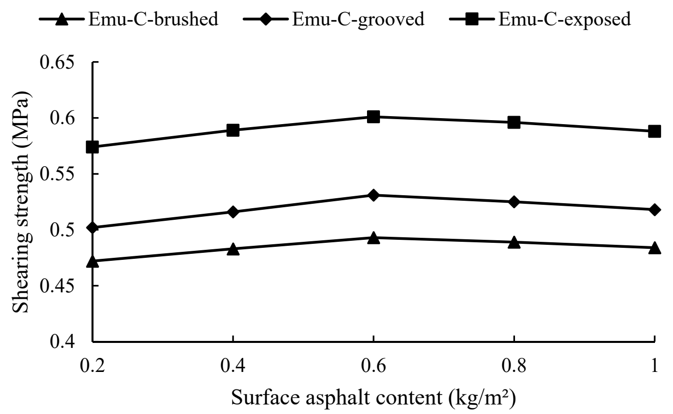

Figure 3. Shear strength of SBS-modified emulsified asphalt under different upper layer asphalt content.

2.3.2. 90 Ordinary Hot Asphalt

90 ordinary hot asphalt was sprayed with areal density of 0.8, 1.0, 1.2, 1.4, and 1.6 kg/m^2, and gravel was sprayed with an areal density of 5.0, 6.0, 7.0, and 8.0 kg/m^2, yield a total of 20 waterproof materials. According to the test scheme Ord-A-brushed, Ord-A-grooved, Ord-A-exposed, Ord-B-brushed, Ord-B-grooved, and Ord-B-exposed, each kind of waterproof adhesive was prepared and direct shear tests were conducted (please refer to Table 1 for details). The experimental results are shown in Figure 4.

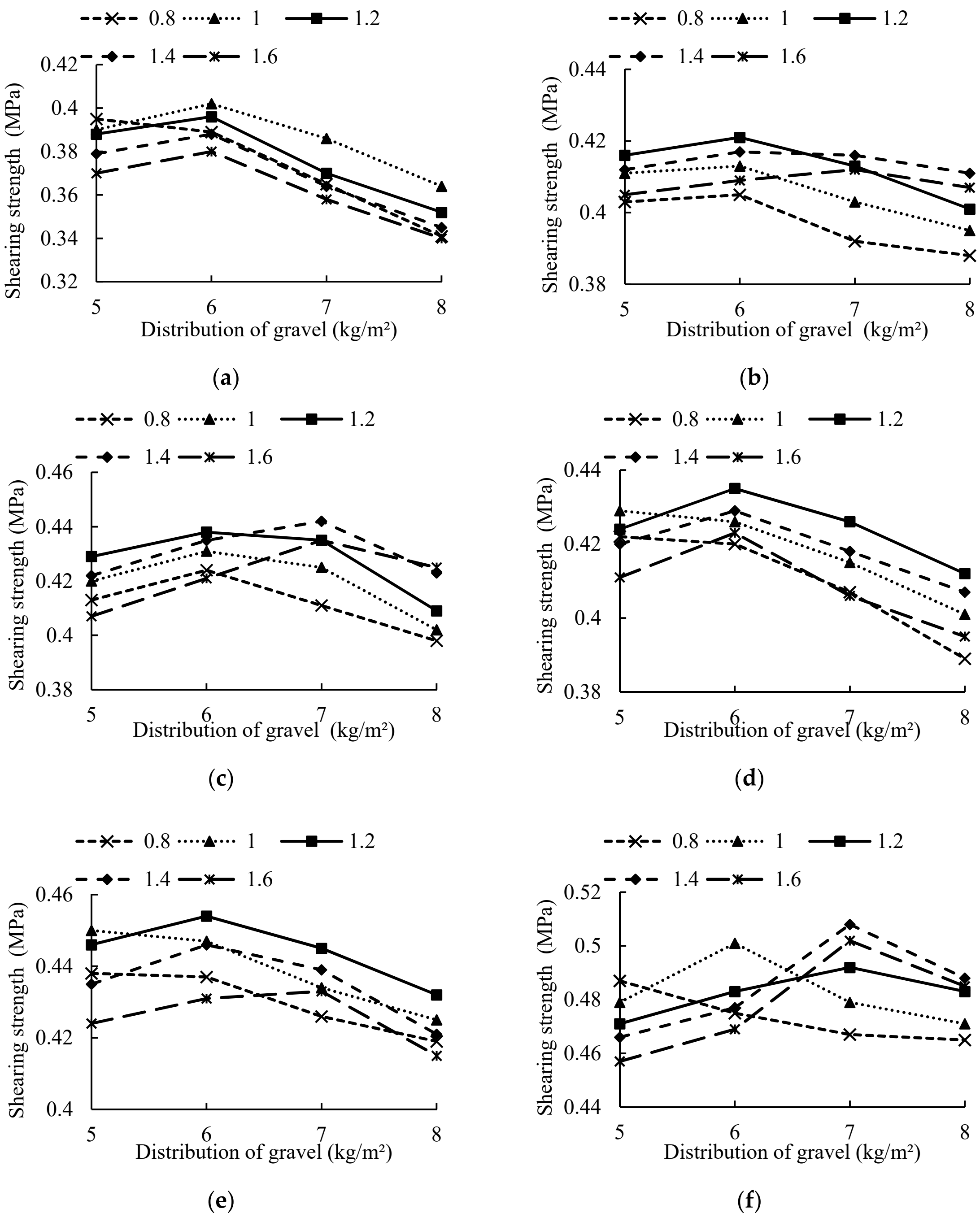

Figure 4. Shear strength of 90 ordinary hot asphalt with different spreading and disposal schemes: (**a**) Ord-A-brushed; (**b**) Ord-A-grooved; (**c**) Ord-A-exposed; (**d**) Ord-B-brushed; (**e**) Ord-B-grooved; (**f**) Ord-B-exposed.

Figure 4 shows that the optimum asphalt and gravel content in scheme Ord-A-brushed is 1.0 kg/m^2 and 6.0 kg/m^2, respectively. The optimum asphalt content in scheme Ord-A-grooved, Ord-B-brushed, and Ord-B-grooved is 1.2 kg/m^2, and the optimum gravel content is 6.0 kg/m^2. The optimum asphalt content in scheme Ord-A-exposed and Ord-B-exposed is 1.4 kg/m^2 and the optimum gravel content is 7.0 kg/m^2.

After determining the optimum content of asphalt and gravel content in scheme A, upper asphalt was sprayed with areal density of 0.2, 0.4, 0.6, 0.8, and 1.0 kg/m^2, which is composed of five kinds of waterproof adhesives. According to the test scheme Ord-C-brushed, Ord-C-grooved, and Ord-C-exposed schemes, each kind of waterproof adhesive was prepared, and direct shear tests were conducted (please refer to Table 1 for details). The test results are shown in Figure 5.

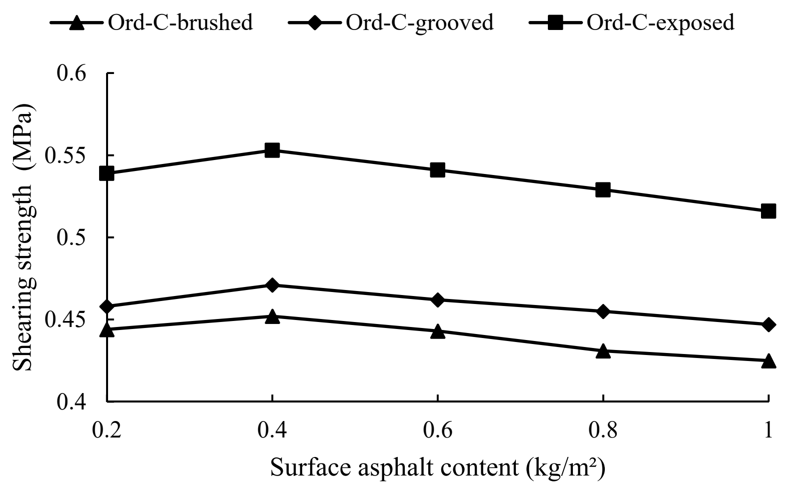

Figure 5. Shear strength of 90 ordinary hot asphalt with different asphalt content in the upper layer.

According to Figure 5, the optimum asphalt content of upper modified asphalt in schemes Ord-C-brushed, Ord-C-grooved, and Ord-C-exposed is 0.4 kg/m^2. The optimum asphalt content in scheme Ord-C-brushed is 0.4 kg/m^2 in the upper layer, 1.0 kg/m^2 in the lower layer, and the optimum gravel content is 6.0 kg/m^2. The optimum asphalt content in scheme Ord-C-grooved is 0.4 kg/m^2 in the upper layer, 1.2 kg/m^2 in the lower layer, and the optimum gravel content is 6.0 kg/m^2. The optimum asphalt content in scheme Ord-C-exposed is 0.4 kg/m^2 in the upper layer, 1.4 kg/m^2 in lower layer, and the optimum gravel content is 7.0 kg/m^2.

2.3.3. SBS-Modified Asphalt

SBS-modified asphalt was sprayed with areal density of 0.8, 1.0, 1.2, 1.4, and 1.6 kg/m^2, and gravel was sprayed with an areal density of 5.0, 6.0, 7.0, and 8.0 kg/m^2, yielding a total of 20 waterproof materials. According to the test scheme Mod-A-brushed, Mod-A-grooved, Mod-A-exposed, Mod-B-brushed, Mod-B-grooved, and Mod-B-exposed, each kind of waterproof adhesives was prepared and direct shear tests were conducted (please refer to Table 1 for details). The experimental results are shown in Figure 6.

Figure 6 shows that the optimum asphalt content in scheme Mod-A-brushed is 1.0 kg/m^2 and the optimum gravel content is 6.0 kg/m^2. The optimum asphalt content in scheme Mod-A-grooved, Mod-B-brushed, and Mod-B-grooved is 1.2 kg/m^2, and the optimum gravel content is 6.0 kg/m^2. The optimum asphalt content in scheme Mod-A-exposed and Mod-B-exposed is 1.2 kg/m^2 and the optimum gravel content is 7.0 kg/m^2.

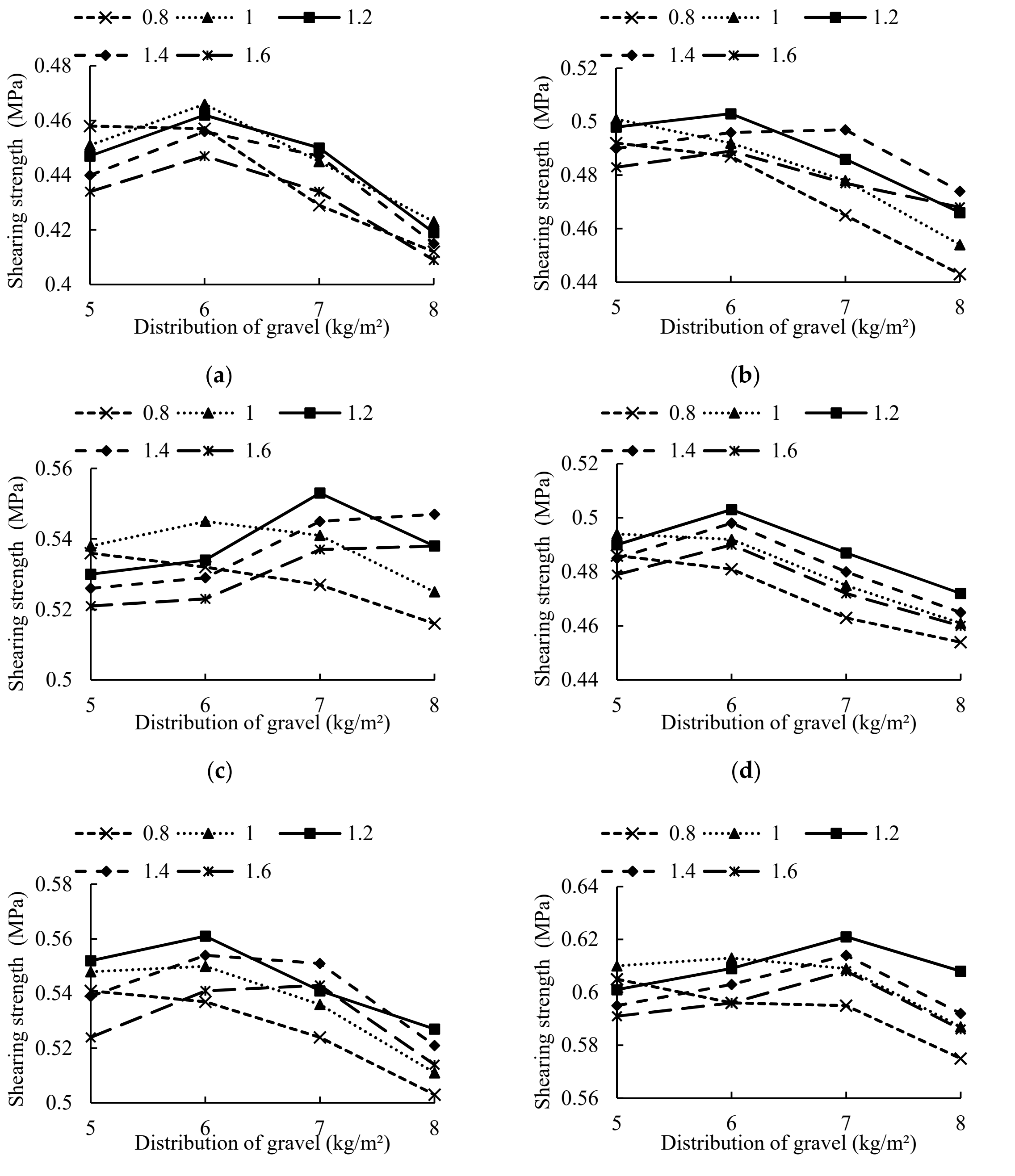

Figure 6. Shear strength of SBS-modified asphalt with different spreading and disposal schemes: (**a**) Mod-A-brushed; (**b**) Mod-A-grooved; (**c**) Mod-A-exposed; (**d**) Mod-B-brushed; (**e**) Mod-B-grooved; (**f**) Mod-B-exposed.

After determining the optimum asphalt and gravel content in scheme A, the upper asphalt was sprayed with an areal density of 0.2, 0.4, 0.6, 0.8, and 1.0 kg/m^2, which is composed of five kinds of waterproof adhesives. According to the test scheme Mod-C-brushed, Mod-C-grooved, and Mod-C-exposed schemes, each kind of waterproof adhesive was prepared, and direct shear tests were carried out (please refer to Table 1 for details). The test results are shown in Figure 7.

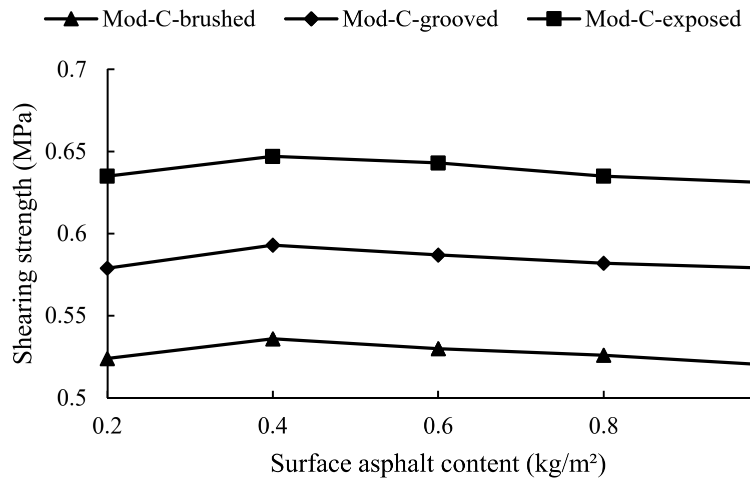

Figure 7. Shear strength of SBS-modified asphalt under different upper layer asphalt content.

From Figure 6, the optimum asphalt content in Mod-C-brushed, Mod-C-grooved, and Mod-C-exposed upper modified asphalt is 0.4 kg/m^2. The optimum asphalt content in scheme Mod-C-brushed is 0.4 kg/m^2 in the upper layer, 1.0 kg/m^2 in the lower layer, and the optimum gravel content is 6.0 kg/m^2. The optimum asphalt content in scheme Mod-C-grooved is 0.4 kg/m^2 in the upper layer, 1.2 kg/m^2 in the lower layer, and the optimum gravel content is 6.0 kg/m^2. The optimum asphalt content in scheme Mod-C-exposed is 0.4 kg/m^2 in the upper layer, 1.2 kg/m^2 in the lower layer, and the optimum gravel content is 7.0 kg/m^2.

2.4. Comparison of Different Waterproof Cohesive Layer Schemes Based on Optimum Material Quantity

The shear strength test results with different waterproof cohesive layers at the optimum asphalt and gravel content are shown in Figure 8.

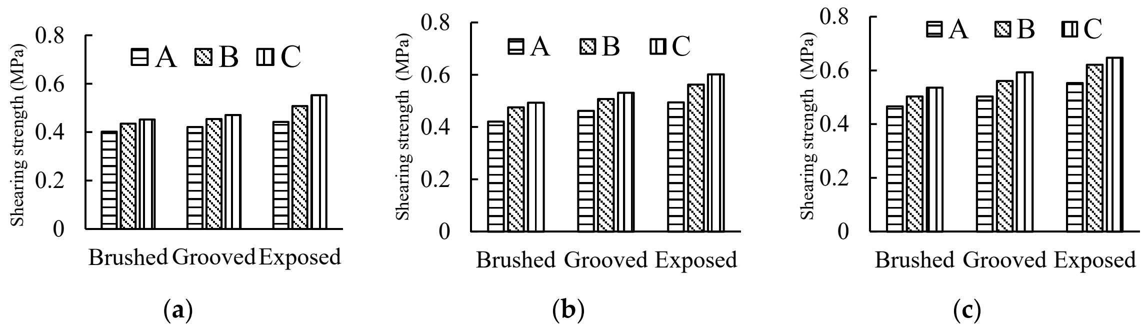

Figure 8. Maximum shear strength of different cement slab surfaces and spreading schemes: (**a**) SBS-modified emulsified asphalt; (**b**) 90 ordinary hot asphalt; (**c**) SBS-modified asphalt.

Figure 8 shows that the surface treatment method with the highest shear strength is exposed aggregate cement concrete, followed by grooved cement concrete and brushed cement concrete. The shear strength of grooved cement concrete is 4% to 12% higher than that of brushed cement concrete, and the shear strength of exposed aggregate cement concrete is 10% to 23% higher than that of brushed cement concrete. The bonding material with the highest shear strength is SBS-modified asphalt, followed by SBS-modified emulsified asphalt and 90 ordinary hot asphalt. The shear strength of SBS-modified emulsified asphalt is 5% to 13% higher than that of 90 ordinary hot asphalt, and the shear strength SBS-modified asphalt is 16% to 32% higher than that of 90 ordinary hot asphalt. Spreading scheme C provides the highest shear strength, followed by spreading scheme B and spreading scheme A. The shear strength provided by spreading scheme B is 4% to 12% higher than that from spreading scheme A, and the shear strength from spreading scheme C is 10% to 23% higher than that from spreading scheme A.

3. Shear Fatigue Characteristics of Waterproof Cohesive Layer Materials

3.1. Test Design

Considering that the bridge deck waterproof cohesive layer material is subjected to repeated shear stresses under actual working conditions and the bridge deck ultimately experiences damage due to shear fatigue, the fatigue life of the bridge deck waterproof cohesive layer material was studied using an electro-hydraulic servo fatigue testing machine [21]. The specimens were prepared as follows: the surface of the board was treated as exposed aggregate cement concrete and spreading scheme C was used. To compare the fatigue properties of different waterproof cohesive layer materials, three kinds of waterproof cohesive layers were designed with the asphalt and gravel content shown in Table 7. Double-layer cylinder specimens of Φ10 cm × 10 cm were used for interlaminar shear fatigue tests. The specific preparation method is the same as that described in Section 2.1 [22]. The forming and testing process of fatigue samples are shown in Figure 9.

Table 7. Waterproof cohesive layer material quantity (kg/m^2).

Material	Lower Asphalt	Stone	Surface Asphalt
SBS-modified emulsified asphalt	1.4	7.0	0.6
90 ordinary hot asphalt	1.4	7.0	0.4
SBS-modified asphalt	1.2	7.0	0.4

(a) (b) (c)

Figure 9. The forming and testing process of fatigue samples: (**a**) electro-hydraulic servo fatigue testing machine; (**b**) the sample forming process; (**c**) direct shear test with vertical load.

In the fatigue test, the cyclic stress ratio $P = P_{max}/P_{min} = 0.1$, P_{max} is the maximum stress, and P_{min} is the minimum stress. The maximum shear strength can be found in Table 8. Loading waveform and frequency is 10 Hz sine wave, loading time is 0.016 s, which is equivalent to a speed of 60–65 km/h [23]. In addition, before starting the test, the specimen is preloaded with the minimum load for more than 10 s, to ensure good contact between the test components. The following parameters were selected for fatigue testing.

Table 8. Shear strength of the waterproof cohesive layer in different interlayer bonding states.

Material	Shear Strength Value (MPa)	Maximum Shear Strength (kN)
SBS-modified emulsified asphalt	1.112	8.5
90 ordinary hot asphalt	1.035	7.8
SBS-modified asphalt	1.128	8.6

(1). Loading mode: stress control (the peak value of the load remains stable until the specimen is destroyed)
(2). Loading waveform and frequency: 10 Hz sine wave
(3). Stress ratio: 0.3 to 0.7 in intervals of 0.1 (0.1 cyclic stress ratio)

3.2. Results

Before conducting the shear fatigue test, and in consideration of the actual interlayer working state of the bridge deck, the interlayer shear strength of specimens with different cohesive layers was obtained by using 0.7 MPa as a standard vertical load in order to determine the stress level of the specimens [24]. The interlayer shear strength of the specimens with different cohesive layers was tested at 15 °C [25]. The experimental results are shown in Table 8.

To eliminate the variability of the test results as far as possible, six groups of parallel tests were conducted with each kind of waterproof cohesive layer material, and the average value was taken as the fatigue life of the cohesive material obtained under the test conditions. The test results are shown in Figure 10.

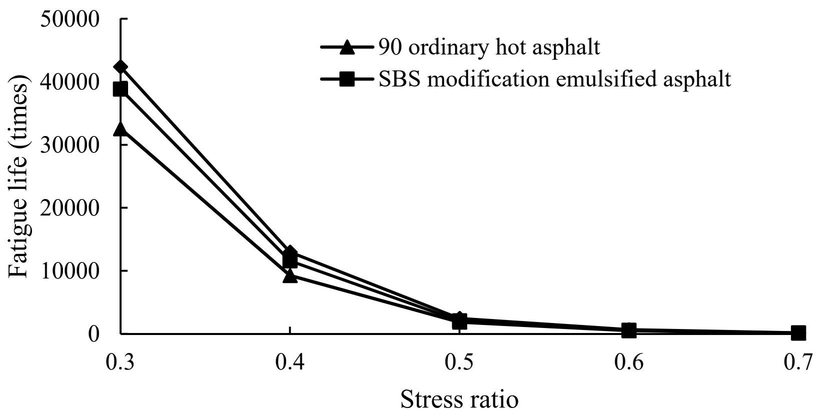

Figure 10. Variation in fatigue life for different waterproof cohesive layer materials with different stress ratios (15 °C).

Figure 8 shows that the shear fatigue life of the different waterproof cohesive layer materials decreases as the stress ratio increases. When the stress ratio was 0.3, the interlaminar shear fatigue life of the SBS-modified emulsified asphalt, 90 ordinary hot asphalt, and SBS-modified asphalt is 38,820, 322,553, and 42,360 repetitions, respectively. When the stress ratio was 0.7, the fatigue life of the three waterproof cohesive layer materials is 139, 110, and 143 repetitions, respectively. The shear fatigue life decreases by about 72% when the stress ratio of 90 ordinary hot asphalt increases from 0.3 to 0.4. When the stress ratio of SBS-modified emulsified asphalt increases from 0.3 to 0.4, the shear fatigue life decreases by about 70%. Meanwhile, when the stress ratio of SBS-modified asphalt increases from 0.3 to 0.4, the shear fatigue life decreases by about 69%. Therefore, changing the stress ratio significantly influences the fatigue life; therefore, overloaded vehicles should be strictly limited in operation to prevent interlayer shear fatigue damage to a bridge deck.

To study the effect of temperature on the shear fatigue properties of waterproof cohesive layer materials, shear fatigue tests were conducted at different temperatures for each waterproof and cohesive layer material. The stress ratio of the test specimens was 0.4. The test results are shown in Figure 11.

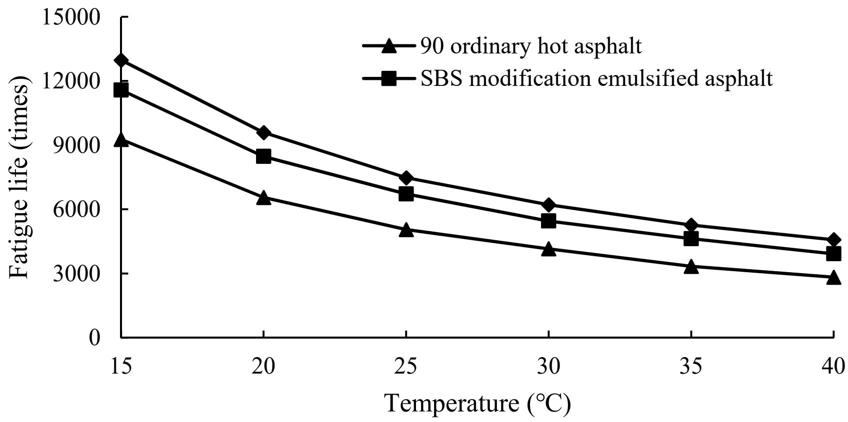

Figure 11. Variation in fatigue life for different waterproof cohesive layer materials at different temperatures.

According to Figure 11, a change in temperature has a significant influence on fatigue life. The fatigue life of all three waterproof cohesive layer materials decreases by about 26%, 20%, and 17% when the temperature increases from 15 to 20 °C, from 20 to 25 °C, and from 25 to 30 °C, respectively.

In summary, SBS-modified asphalt has the longest shear fatigue life, followed by SBS-modified emulsified asphalt and 90 ordinary hot asphalt. Li et al. [26] carried out high-speed shear tests on SBS-modified asphalt at 170–180°C. The test results show that the elastic recovery rate of SBS-modified asphalt is higher than that of 90 ordinary hot asphalt, so the deformation of SBS-modified asphalt is smaller, the recovery rate is faster, and the numbers of load actions and fatigue life it can bear are larger than that of 90 ordinary hot asphalt. However, the addition of emulsifier will affect the change of properties of SBS-modified asphalt and result in the weakening of related performance indexes, but the performance of SBS-modified emulsified asphalt is still improved compared with 90 ordinary hot asphalt. This is consistent with the results of Figures 10 and 11.

3.3. Indoor Shear Fatigue Equation

According to the laboratory test results, the fatigue life diagram of the waterproof cohesive layer material at 15 °C is a logarithmic function of shear stress ($lg\tau$), where the logarithmic fatigue life $\lg N_f$ is the ordinate, as shown in Figure 12.

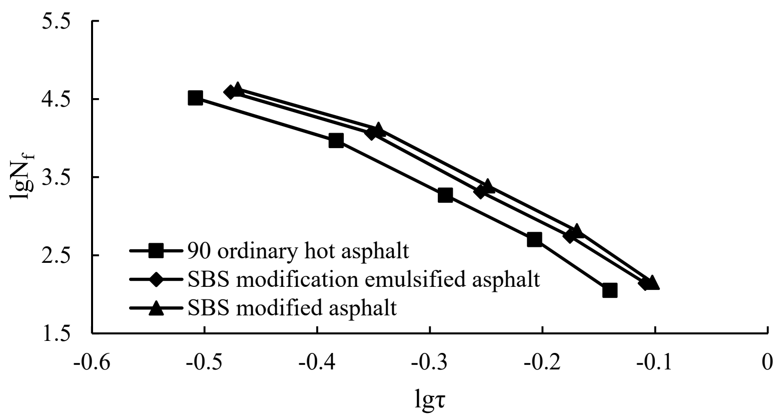

Figure 12. Relationship between fatigue life and stress ratio for different waterproof cohesive layer materials.

The logarithmic shear stress-fatigue life equations for different waterproof cohesive layer materials were obtained using linear regression in MATLAB, and the results are shown in Table 9.

Table 9. Shear fatigue equations for different waterproof cohesive layer materials.

Material	Shear Fatigue Equation	Prediction Model	Coefficient of Determination
SBS-modified emulsified asphalt	$\lg N_f = 1.536 - 6.704 \lg\tau$	$N_f = 34.38\tau^{-6.704}$	0.982
90 ordinary hot asphalt	$\lg N_f = 1.265 - 6.675 \lg\tau$	$N_f = 18.42\tau^{-6.675}$	0.980
SBS-modified asphalt	$\lg N_f = 1.623 - 6.719 \lg\tau$	$N_f = 41.97\tau^{-6.719}$	0.977

When the shear stress between decks is determined, the fatigue life of different waterproof cohesive layer materials (15 °C) can be predicted using the indoor shear fatigue life model shown in Table 9.

According to Figure 11, changing the temperature influences the fatigue life; thus, it is necessary to modify the fatigue equation of the waterproof cohesive layer to accommodate temperature changes [27]. Fitting the data in Table 10 to a power function shows a strong correlation between N_{fT}/N_{fT0} and T/T_0, where N_{fT} is the shear fatigue life at temperature T and N_{fT0} is the shear fatigue life at 15 °C.

Table 10. Temperature correction coefficient for the fatigue life model.

Test Temperature (°C)	T/T_0	N_{fT}/N_{fT0}		
		SBS-Modified Emulsified Asphalt	90 Ordinary Hot Asphalt	SBS-Modified Asphalt
15	1.00	1.000	1.000	1.000
20	1.33	0.732	0.707	0.739
25	1.67	0.581	0.545	0.576
30	2.00	0.471	0.448	0.479
35	2.33	0.400	0.360	0.406
40	2.67	0.339	0.305	0.353
$\log_{(T/T_0)}\left(N_{fT}/N_{fT0}\right)$		−1.10	−1.20	−1.06

The modified coefficient is introduced into the shear fatigue life prediction equation, and the modified shear fatigue life prediction equation of waterproof cohesive layer material at different temperatures is shown in Table 11.

Table 11. Shear fatigue life prediction model for waterproof cohesive layer materials with temperature correction.

Material	Prediction Model
SBS-modified emulsified asphalt	$N_f = 34.38\tau^{-6.704}\left(\frac{T}{T_0}\right)^{-1.10}$
90 ordinary hot asphalt	$N_f = 18.42\tau^{-6.675}\left(\frac{T}{T_0}\right)^{-1.20}$
SBS-modified asphalt	$N_f = 41.97\tau^{-6.719}\left(\frac{T}{T_0}\right)^{-1.06}$

3.4. Equivalent Temperature Calculation

According to the fatigue equations shown in Table 11, the relationship between the interlaminar shear fatigue life of the waterproof cohesive layer, applied stress, and its temperature can be expressed as the following function of shear stress and temperature:

$$N_f = X_N\left(\frac{1}{\tau}\right)^{Y_N}\left(\frac{1}{T}\right)^{Z_N} \tag{1}$$

where X_N, Y_N, and Z_N are regression coefficients.

Miner's linear cumulative damage theory [28,29] can be used to express the accumulated fatigue damage, as shown in Equation (2):

$$D = \sum_{\mathrm{i}=1}^{\mathrm{m}} \frac{n_i}{N_i} \tag{2}$$

where D is the cumulative fatigue damage rate, Ni is the number of repetitions corresponding to loads at various loads during material failure, and n_i is the number of loads at various levels in practice.

The shear stress and shear strength will change due to variations in the temperature distribution $T(z,t)$ of the bridge deck [30]. According to the integral mean value theorem, there must be an equivalent temperature T_{eq} in the temperature field. At this temperature, the shear fatigue life of the bridge deck interlayer material is N_{eq}, and there exists $D = D_{eq} = \sum_{i=1}^{m} \frac{n_i}{N_{eq}}$, i.e., $N_{eq} = \frac{\sum_{i=1}^{m} n_i}{D}$.

It is difficult to accurately predict the vehicle load distribution at a certain temperature T_i. To simplify the calculation, it is assumed that the axle loads are uniformly distributed at all time periods, and the horizontal shear stress on the waterproof cohesive layer material does not change with temperature [31], as defined in Equation (3):

$$n_i = N \times f_i \tag{3}$$

where n_i is the number of standard axle loads at temperature T_i, f_i is the distribution frequency at the tack coat temperature T_i during the design period, and N is the cumulative frequency of standard axle loads on the asphalt pavement during the design period.

Equation (4) can be obtained by substituting Equations (2) and (3) into $N_{eq} = \frac{\sum_{i=1}^{m} n_i}{D}$:

$$N_{eq} = \frac{\sum_{i=1}^{m} n_i}{D} = \frac{\sum_{i=1}^{m} N \times f_i}{\sum_{\mathrm{i}=1}^{\mathrm{m}} \frac{\mathrm{n_i}}{\mathrm{N_i}}} = \frac{\sum_{i=1}^{m} N \times f_i}{\sum_{\mathrm{i}=1}^{\mathrm{m}} \frac{N \times f_i}{\mathrm{N_i}}} = \frac{1}{\sum_{\mathrm{i}=1}^{\mathrm{m}} \frac{f_i}{\mathrm{N_i}}} = X_N \left(\frac{1}{\tau}\right)^{Y_N} \left(\frac{1}{T_{eq}}\right)^{Z_N} \tag{4}$$

Further reduction yields Equation (5):

$$T_{eq} = \left(\sum_{i=1}^{m} {T_i}^{Z_N} \times f_i\right)^{\frac{1}{Z_N}} \tag{5}$$

According to Equation (5), the equivalent temperature T_{eq} of the bridge deck interlaminar shear fatigue can be calculated from the temperature T_i and its distribution frequency f_i during the design service life.

4. Bridge Deck Waterproof Cohesive Layer Interlayer Design Method

When designing the deck pavement layer, there is no special axle load pavement conversion method, and the traffic volume conversion still uses the conversion formula from asphalt pavement design [32]. The interlayer shear fatigue design index for a waterproof cohesive layer in a bridge deck increased in this study, and engineering examples were used for verification. The design criteria for shear fatigue are shown in Equation (6):

$$N_f \geq N_e \tag{6}$$

where N_f is the shear fatigue life and N_e is the accumulated number of equivalent applied axle loads in the design lane during the design period.

4.1. Axle Load Conversion Method Based on Shear Fatigue Damage

Converting the number of actions between different axle loads follows the principle of equivalence, i.e., the bridge deck pavement structure calculated according to the design index with different converted different axle loads is always the same [33]. Therefore, one can derive an equation for converting the shear stress between the waterproof cohesive layers of the bridge deck to an axle load, allowing the design index to be determined.

The axle load conversion method for a bridge deck pavement system based on fatigue equivalence is as follows: BZZ-100 (horizontal force coefficient f is taken as 0.15) is used as the standard axle load based on bond shear fatigue axle load conversion [34]. The maximum interlaminar shear stress ratio with different axle loads is defined [35] in Equation (7):

$$\frac{\tau_{xy1}}{\tau_{xy2}} = \left(\frac{P_1}{P_2}\right)^b \tag{7}$$

According to the shear fatigue test results for waterproof bonding materials, the relationship between shear fatigue life of the bonding materials and interlaminar shear stress can be expressed as shown in Equation (8):

$$N = X_N \tau^{-Y_N} \tag{8}$$

Based on the principle of equivalence for axle load conversion, the shear stress ratio under different axial loads is shown in Equation (9):

$$\frac{\tau_1}{\tau_2} = \left(\frac{N_1}{N_2}\right)^{-\frac{1}{Y_N}} \tag{9}$$

Equation (10) can be obtained by combining Equations (7) and (9), where bY_N is equivalent axle load conversion factor:

$$\frac{N_1}{N_2} = \left(\frac{P_2}{P_1}\right)^{bY_N} \tag{10}$$

The different axle load ratios and their corresponding maximum shear stress ratios can be calculated, and regression can be used to determine the average standard axle load conversion index b. Here, we determined b = 0.53. The fatigue life equation for different bonding materials was presented in Section 3.3, and the exponent Y_N can be determined. The bY_N values for different bonding materials are shown in Table 12.

Table 12. bY_N values for different bonding materials.

Material	SBS-Modified Emulsified Asphalt	90 Ordinary Hot Asphalt	SBS-Modified Asphalt
Y_N	6.704	6.675	6.719
bY_N	3.55	3.54	3.56

To ensure that the axle load conversion result is reliable, bY_N = 3.6 was selected as the equivalent axle load conversion factor for designing waterproof cohesive materials to prevent interlayer shear fatigue. The calculated result is smaller than the current asphalt pavement conversion index of 4.35 according to the deflection axis; thus, axle load changes have less influence on the interlayer than on permanent deformation and fatigue cracking in the pavement.

4.2. Design Method of Waterproof Cohesive Layer

The bridge deck waterproof cohesive layer is designed with the fatigue damage to the bonding material as the design index. N_e is calculated from the traffic volume and the fatigue equivalence principle of the bonding material:

$$N_e = \frac{\left|(1+\gamma)^t - 1\right| \times 365}{\gamma} N_1 \times \mathrm{F} \tag{11}$$

where γ is the average annual growth rate of traffic volume, t is the design cycle, N_1 is the average daily equivalent axis in the design lane in the first year, and F is the brake reduction factor (F = 0.1 for a special road and F = 0.05 for a general road). N_1 in Equation (11) is defined as follows:

$$N_1 = \sum_{i=1}^{K} n_i C_1 C_2 \left(\frac{P_i}{P}\right)^{bY_N} \tag{12}$$

where n_i is the axle load from converted vehicles at different traffic volumes, P is a standard axle load, P_i is the axle load for a converted vehicle, K is the number of different vehicles converted, C_1 is an axle number coefficient, C_2 is a wheel group coefficient, and bY_N = 3.6.

The maximum longitudinal shear stress τ at the interlayer position under the standard load is then calculated. The equivalent shear fatigue temperature T_{eq} can be determined with Equation (5) using local atmospheric temperature data. The fatigue life N_f can be determined from test results with different treatment schemes for the waterproof cohesive layer such that $N_f \geq N_e$, where N_e is calculated using Equation (11). The aforementioned inequality ensures the treatment method for the waterproof cohesive layer meets the design requirements; otherwise, the treatment method must be redesigned.

4.3. Design Example

Taking the cement concrete bridge around the southern city of Ulanchabu in Inner Mongolia as an example, the bridge is a two-way, four-lane road with a bridge deck thickness of 10 cm and a design life of 12 years. The average annual growth rate of traffic volume is 6%. According to the fatigue equivalent principle of the bonding material, N_1 is 4690 repetitions/day, and N_e is 1.44 million repetitions.

Air temperature was provided by the National Meteorological Information Center of China Meteorological Administration (http://data.cma.cn/), and frequency data for the air temperature distribution was determined statistically, as shown in Table 13.

Table 13. Frequency data for air temperature distribution in Ulanchabu.

Temperature Range (°C)	−30 to −20	−20 to −10	−10 to 0	0 to 10	10 to 20	20 to 25	25 to 30	30 to 35
Distribution Frequency	0.04	0.14	0.21	0.25	0.19	0.09	0.06	0.02

To determine the effect of temperature on shear fatigue failure, the relationship between the temperature field and the temperature at different depths into the bridge deck pavement was obtained based on research results from Yu and Zheng [36], as shown in Equation (13):

$$T_d = 0.91T_a - 0.21d + 4.84 \tag{13}$$

where T_d is the temperature of deck pavement structure (°C) at an arbitrary depth d, T_a is the atmospheric temperature (°C), and d is the distance from any position on the bridge deck pavement structure to the road surface (cm).

The temperature distribution at the interlayer position of the bridge deck was calculated using the prediction model for the temperature field and atmospheric temperature distribution. To simplify the calculation, 10 °C was taken as the representative temperature when the atmospheric temperature was lower than 10 °C. In other temperature ranges, the intermediate temperature within the temperature range was used as the representative value. The representative values were used in Equation (13) to calculate the temperature and frequency at the interlayer position of the bridge deck. The calculation results are shown in Table 14.

Table 14. Representative temperature distribution frequency between decks in Ulanchabu.

Interlayer Temperature (°C)	11.8	16.4	23.2	27.8	32.3
Distribution Frequency	0.64	0.19	0.09	0.06	0.02

The correction coefficient Z_N for the shear fatigue temperature for different waterproof cohesive layer materials and the data in Table 14 were substituted into Equation (5) in order to calculate the equivalent interlaminar shear fatigue temperature. The equivalent temperatures of different waterproof cohesive layer materials were calculated and are shown in Table 15.

Table 15. Equivalent temperatures of different waterproof cohesive layer material.

Material	Z_N	T_{eq} (°C)
SBS-modified emulsified asphalt	1.10	15.15
90 ordinary hot asphalt	1.20	15.24
SBS-modified asphalt	1.06	15.12

Table 15 shows that the equivalent temperatures calculated for different waterproof cohesive layer materials are different, but they are all near 15 °C. This is because the shear fatigue lives of different waterproof cohesive layer materials have different sensitivities to temperature, but the equivalent temperature depends more on the local temperature distribution frequency and has little correlation with material.

Considering that the indoor fatigue test is continuous loading, the shear deformation is not constrained, but the actual situation is that the pavement layers are constrained, and the driving load is intermittent. Therefore, considering the influence factors such as load intermittence time, crack propagation time, transverse distribution of wheel load, refer to Pell's research [37,38], according to the indoor shear fatigue equation for different materials obtained in Table 11, the actual shear fatigue equation is expanded by 100 repetitions [39], as shown in Table 16.

Table 16. Predicted shear fatigue life for different waterproof cohesive layer materials at 15 °C (0.4 MPa interlayer shear stress).

Material	Prediction Model	N_e
SBS-modified emulsified asphalt	$N_f = 100 \times 34.38\tau^{-6.704}\left(\frac{T_{eq}}{T_0}\right)^{-1.10} = 158 \times 10^4$	144×10^4
90 ordinary hot asphalt	$N_f = 100 \times 18.42\tau^{-6.675}\left(\frac{T_{eq}}{T_0}\right)^{-1.20} = 82 \times 10^4$	
SBS-modified asphalt	$N_f = 100 \times 41.97\tau^{-6.719}\left(\frac{T_{eq}}{T_0}\right)^{-1.06} = 196 \times 10^4$	

One can see that the interlaminar shear fatigue check of 90 ordinary hot asphalt does not meet the design requirements, while the interlayer fatigue of SBS-modified emulsified asphalt and SBS-modified asphalt meet the design requirements. Therefore, when fatigue cracking and permanent deformation of the traditional asphalt layer are taken as the design indices, the fatigue characteristics of interlaminar materials are not taken into account. It is recommended that the interlayer shear fatigue design index be increased when designing a waterproof cohesive layer for a bridge deck.

5. Conclusions

Indoor shear tests were used to determine the shear strength of different slab disposal schemes for cement slabs (brushed cement concrete, grooved cement concrete, and exposed aggregate cement concrete), waterproof cohesive layer materials (SBS-modified emulsified asphalt, 90 ordinary hot asphalt, and SBS-modified asphalt), and different combinations of spreading schemes. The optimum material composition for the waterproof cohesive layer was presented.

The influence of shear stress and temperature on the fatigue life of the waterproof cohesive layer was determined from indoor shear fatigue tests. The shear fatigue life of the waterproof cohesive layer material decreases by more than 70% when the stress ratio increases by only 0.1, and the fatigue life of the waterproof cohesive layer material decreases by more than 20% when the temperature increases by 5 °C.

An equation for predicting the indoor shear fatigue of a waterproof cohesive layer material at 15 °C was established, and temperature correction was applied. Based on the temperature distribution in the cement concrete bridge deck, a method for calculating the equivalent temperature T_{eq} of the interlayer shear fatigue of the bridge deck using the distribution frequency f_i of temperature T_i during service is proposed.

The design method and design index for a bridge deck considering shear fatigue damage between the waterproof cohesive layers were discussed. The application results show that the interlayer contact does not meet the shear fatigue requirements when fatigue cracking and permanent deformation of a traditional asphalt layer are taken as design indices and when fatigue of the interlaminar materials are not considered. Therefore, the design index of the interlayer shear fatigue should be proposed.

Author Contributions: Conceptualization, X.W. and N.F.; methodology, N.F. and Z.S.; formal analysis, H.Y. and Y.S.; investigation, N.F. and Y.S.; resources, X.W.; data curation, N.F. and H.Y.; writing—original draft preparation, N.F. and L.Y.; writing—review and editing, N.F., X.W., H.Y. and Z.S.; visualization, N.F., X.W., H.Y. and L.Y.; supervision, X.W.; funding acquisition, X.W.

Funding: This research was funded by Construction of science and technology projects by Ministry of Communications of China (2013 318 J08 220), and the Inner Mongolia Autonomous Region transportation science and technology project of China (NJ-2018-23).

Conflicts of Interest: The authors declare no conflicts of interest.

References

1. Hu, C.H.; Qian, J. Shear Stress Analysis of Long-span Steel Bridge Deck Asphalt Pavement using FEM. *Adv. Mater. Res. Sci.* **2011**, *304*, 12–17. [CrossRef]
2. Wang, L.B.; Hou, Y.; Zhang, L.; Liu, G.J. A combined static-and-dynamics mechanics analysis on the bridge deck pavement. *J. Clean. Prod. Sci.* **2017**, *166*, 209–220. [CrossRef]
3. Mitchell, M.R.; Link, R.E.; Zhou, Q.H.; Xu, Q.W.; Zhang, Z.J. Measurements with a New Peel Adhesion Test on Waterproof Membranes Used on Concrete Bridge Decks. *Astron. Astrophys. Sci.* **2008**, *36*, 89–93. [CrossRef]
4. Ai, C.F.; Rahman, A.; Wang, F.Y.; Yang, E.H.; Qiu, Y.J. Experimental study of a new modified waterproof asphalt concrete and its performance on bridge deck. *Road Mater. Pavement Sci.* **2017**, *18*, 270–280. [CrossRef]
5. Yu, X.G.; Wang, B.P.; Chen, L.L.; You, M.H.; Luo, R. Study on Shear Resistance of Waterproof Bonding Layer of Bridge Deck Pavement Based on MTS. *J. Wuhan Univ. Technol.* **2017**, *41*, 484–487.
6. Zhou, S.L.; Zhu, F.; Wu, B.; Cheng, Y.Z.; Yang, K. Experimental study on mechanical properties of waterproof bonding materials for bridge deck pavement. *Chin. Foreign Highway* **2014**, *34*, 272–275.
7. Oscarsson, E.; Said, S. Assessment of ZSV in asphalt concrete using shear frequency sweep testing. *J. Mater. Civil Eng. Sci.* **2012**, *24*, 1305–1309. [CrossRef]
8. West, R.C.; Moore, J.R.; Zhang, J.N. Evaluation tack coat applications and the bond strength between pavement layers. In Proceedings of the American Society of Civil Engineers Airfield and Highway Pavements Specialty Conference, Atlanta, GA, USA, 30 April–3 May 2006; pp. 578–588.
9. Ye, F.; Zhou, K.; Jia, X.Y.; Lu, Q.Q.; Yan, J. Evaluation of Shear Performance of Flexible Waterproof-adhesive Layer in Concrete Bridge Pavement Based on Grey Correlation Analysis. *Road Mater. Pavement Sci.* **2009**, *10*, 349–360.
10. Song, J.H.; Wang, L.X.; Tian, J.T.; Chen, F.T. Test study on properties of cohesive materials on bridge deck asphalt pavement. *J. Highway Transp. Res. Dev.* **2008**, *2*, 55–58, 63.
11. Lv, D.W.; He, J.; Sun, X.L. Indoor study on road performance of macromolecule polymer bitumen waterproof and cohesive layer (PCMA). *Adv. Mater. Res. Sci.* **2014**, *912*, 172–177. [CrossRef]

12. Wang, J. Study on Performance of Waterproof Bonding Layer for Asphalt Concrete Pavement on Cement Concrete Bridge Deck. Master's Thesis, Dongnan Unversity, Changsha, China, 2003.
13. Wang, C.F. Study on Application Technology of Waterproof Materials for Bridge Deck Based on Polymer. Master's Thesis, Changan Unversity, Changsha, China, 2006.
14. Ji, L.; Li, Y.; Wang, H.P.; Zhang, L. Shear resistance performance evaluations of rubber asphalt waterproof adhesive layer on bridge deck. In Proceedings of the American Society of Civil Engineer's International Symposium of Climatic Effects on Pavement and Geotechnical Infrastructure, Fairbanks, Alaska, 4–7 August 2013.
15. Rhee, J.; Kim, H.; Ock, C.; Choi, J. An investigation of the deterioration characteristics of concrete bridge decks with asphalt concrete in Korea. *KSCE J. Civ. Eng. Sci.* **2017**, *22*, 613–621. [CrossRef]
16. West, R.C.; Zhang, J.; Moore, J. *Jason Moore Evaluation of Bond Strength Between Pavement Layers*; NCAT Report; National Center for Asphalt Technology: Album, AL, USA, 2005.
17. Hailesilassie, B.W.; Hean, S.; Partl, M.N. Testing of blister propagation and peeling of orthotropic bituminous waterproofing membranes. *Mater. Struct. Sci.* **2015**, *48*, 1095–1108. [CrossRef]
18. Waterproofing Membranes for Concrete Bridge Decks. Available online: https://www.rms.nsw.gov.au/business-industry/partners-suppliers/documents/technical-directions/bpmp2003_02.pdf?tdsourcetag=s_pcqq_aiomsg (accessed on 9 April 2019).
19. Wang, C.H.; Yang, X.; Li, Q.; Guo, T.T.; Jiang, T.T. Preparation and Performance of Conductive Gussasphalt Concrete. *Transportmetrica A* **2018**, *14*, 1–16. [CrossRef]
20. Zhang, Z.Q.; Tao, J.; Zhang, S.T. Experiment and evaluation on performance of epoxy asphalt waterproof cohesive layer on bridge deck pavement. *J. Chang An. Univ. Nat. Sci. Ed.* **2011**, *31*, 1–6.
21. Wang, X.C.; Wang, C.H.; Zhang, Y.P. Research and Development of Interlayer Processing Technology of Combining Pavement. *Road Mach. Constr. Mech.* **2008**, *25*, 9–12.
22. Wang, X.C.; Liu, K.; Li, S.Q. Study on Resistance to Reflective Crack of Interlayer Materials in Asphalt Overlay. *J. Build. Mater.* **2010**, *13*, 247–252.
23. Xie, D.P.; Qi, L. Fatigue performance of asphalt concrete pavement on steel bridge deck. *J. North. Transp.* **2018**, *11*, 38–41.
24. Tajdini, M.; Rostami, A.; Karimi, M.M.; Taherkhani, H. Evaluation of the geo-mechanical parameters of the interface between asphalt concrete and sand with applying direct shear test and numerical modeling. *Adv. Mater. Res. Sci.* **2012**, *587*, 116–121. [CrossRef]
25. Harbin University of Architecture. *Asphalt Pavement Design Indicators and Parameters*; Harbin University of Architecture: Harbin, China, 1993.
26. Li, Z.J.; Zhang, Q.M.; Cheng, G.X. Study on microstructure and properties of SBS modified asphalt during chemical crosslinking. *Contemp. Chem. Ind.* **2007**, *36*, 339–346.
27. Bae, A.; Mohammad, L.N.; Elseifi, M.A.; Button, J.; Patel, N. Effects of Temperature on Interface Shear Strength of Emulsified Tack Coats and Its Relationship to Rheological Properties. Transport. *Res. Rec. Sci.* **2010**, *2180*, 102–109. [CrossRef]
28. Konečný, P.; Lehner, P. Durability assessment of concrete bridge deck considering waterproof membrane and epoxy-coated reinforcement. *Perspect. Sci. Sci.* **2005**, *7*, 222–227. [CrossRef]
29. Tanaka, T.; Kamada, O.; Maruyama, A. Development of asphalt pavement with waterproof performance on concrete slab bridge. *J. Jpn. Soc. Civ. Eng. Ser. E1* **2016**, *72*, 69–75.
30. Xu, D.P.; Feng, X.T.; Cui, Y.J. A Simple Shear Strength Model for Interlayer Shear Weakness Zone. *Eng. Geol. Sci.* **2012**, *147*, 114–123. [CrossRef]
31. Chen, J.S.; Huang, C.C. Effect of Surface Characteristics on Bonding Properties of Bituminous Tack Coat. *Transp. Res. Rec. Sci.* **2010**, *2180*, 142–149. [CrossRef]
32. Chun, S.H.; Kim, K.J.; Greene, J. Evaluation of interlayer bonding condition on structural response characteristics of asphalt pavement using finite element analysis and full-scale field tests. *Constr. Build. Mater. Sci.* **2015**, *96*, 307–318. [CrossRef]
33. Liu, L.P.; Peng, Y.C.; Jing, S. Study on essential performance of waterproof material on concrete bridge deck. *J. Build. Mater.* **2010**, *13*, 48–51.
34. Ye, H.Y.; Wang, X.C.; Fang, N.R.; Su, Z.Y. Low-Temperature Performance and Evaluation Index of Gussasphalt for Steel Bridge Decks. *Adv. Mater. Sci. Eng. Sci.* **2019**. [CrossRef]

35. Wang, X.C.; Su, Z.Y.; Xu, A.M.; Zhou, A.G.; Zhang, H.T. Shear fatigue between asphalt pavement layers and its application in design. *Constr. Build. Mater. Sci.* **2017**, *135*, 297–305. [CrossRef]
36. Yu, Q.L.; Zheng, N.X. Analysis of Temperature Field of Asphalt Mixture Bridge Deck Pavement on Cement Concrete in Urumqi. *J. Wuhan Univ. Technol.* **2012**, *34*, 49–52.
37. Chen, J.; Huang, X.M. Fatigue performance of old asphalt mixture after overlay. *J. Southeast Univ. Nat. Sci. Ed.* **2008**, *3*, 516–519.
38. Ministry of Communications of the People's Republic of China. *JTG D50 Specifications for Design of Highway Asphalt Pavement*; China Communications Press: Beijing, China, 2006.
39. Wang, X.C.; Fang, N.R.; Ye, H.Y.; Zhao, J. Fatigue Damage Analysis of Cement-Stabilized Base under Construction Loading. *Appl. Sci.* **2018**, *11*, 2263. [CrossRef]